Transcriptome analysis reveals key pathways that vary in patients with paroxysmal and persistent atrial fibrillation

HAOLIANG SUN and YONGFENG SHAO

Department of Cardiovascular Surgery, The First Affiliated Hospital of Nanjing Medical University, Nanjing, Jiangsu 210029, P.R. China

Received November 25, 2020; Accepted February 25, 2021

DOI: 10.3892/etm.2021.10003

Abstract. The present study evaluated mRNA and long non-coding RNA (lncRNA) expression profiles and the pathways involved in paroxysmal atrial fibrillation (ParoAF) and persistent atrial fibrillation (PersAF). Nine left atrial appendage (LAA) tissues collected from the hearts of patients with AF (patients with ParoAF=3; and patients with PersAF=3) and healthy donors (n=3) were analyzed by RNA sequencing. Differentially expressed (DE) mRNAs and lncRNAs were identified by $|Log_2$ fold change$|>2$ and $P<0.05$. Gene Ontology (GO), Kyoto Encyclopedia of Genes and Genomes pathway enrichment, protein-protein interaction network and mRNA-lncRNA interaction network analyses of DE mRNA and mRNA at the upstream/downstream of DE lncRNA were conducted. A total of 285 and 275 DE mRNAs, 575 and 583 DE lncRNAs were detected in ParoAF and PersAF samples compared with controls, respectively. PI3K/Akt and transforming growth factor-β signaling pathways were significantly enriched in the ParoAF_Control and the calcium signaling pathway was significantly enriched in the PersAF_Control. *Cis* and *trans* analyses revealed some important interactions in DE mRNAs and lncRNA, including an interaction of *GPC-AS2* with dopachrome tautomerase, and phosphodiesterase 4D and cAMP-specific with *XLOC_110310* and *XLOC_137634*. Overall, the present study provides a molecular basis for future clinical studies on ParoAF and PersAF.

Introduction

Atrial fibrillation (AF) is the most common type of arrhythmia and afflicts numerous individuals worldwide. AF increases the probability of thromboembolism, ischemic stroke, congestive heart failure, psychological distress and death (1). AF impairs patient quality of life (2-4), especially those who require open-heart surgery (5). AF occurs alone or concomitantly with other cardiovascular diseases including valvular heart, coronary artery disease, hypertension and congestive heart failure (6).

AF usually begins in a self-terminating paroxysmal form (ParoAF, defined by episodes lasting <7 days). Over time, the AF pattern often evolves to become persistent (PersAF, duration of episodes >7 days) and non-terminating within 7 days (7). Significant differences exist between ParoAF and PersAF in terms of clinical features, responsiveness to antiarrhythmic drugs and ablation therapy (8). However, the underlying molecular mechanism of the occurrence and development of AF is poorly understood, as well as factors regulating the progression from ParoAF to PersAF.

Gene expression changes are associated with the progression from ParoAF to PersAF (9,10). Studies have primarily focused on the association between microRNAs (miRNAs/miRs) and AF. Several have revealed that miRNAs regulate AF or other cardiovascular diseases by promoting electrical or structural remodeling of the atrium (11-13). Dawson *et al* (11) reported that miR29 likely regulates atrial fibrotic remodeling and may represent a biomarker and/or therapeutic target. In recent years, long non-coding RNAs (lncRNAs), which are longer than 200 nt in length with a nonprotein-coding function, and mRNA expression have gained interest among researchers (14,15). lncRNA plays a central role in many processes during heart development and various heart diseases, including cardiac hypertrophy, cardiac fibrosis, AF and heart failure (16-21). lncRNA AK055347 was upregulated in AF and shown to regulate mitochondrial energy production in myocardiocytes (18). Several mRNAs were demonstrated to be contributed to ParoAF pathogenesis via the gonadotropin releasing hormone receptor and p53 pathways (22). However, these molecular markers were investigated either on patients with ParoAF or PersAF. Few studies have been performed on the differences in the molecular mechanism of patients with ParoAF and PersAF.

In the present study, RNA sequencing (RNA-Seq) technology was used to identify mRNAs and lncRNAs associated with ParoAF and PersAF and to explore the underlying disease mechanisms. Differentially expressed mRNAs (DE mRNAs) and lncRNAs (DE lncRNAs) in ParoAF and

Correspondence to: Professor Yongfeng Shao, Department of Cardiovascular Surgery, The First Affiliated Hospital of Nanjing Medical University, 300 Guangzhou Road, Nanjing, Jiangsu 210029, P.R. China
E-mail: shaoyongfeng_2019@163.com

Key words: paroxysmal atrial fibrillation, persistent atrial fibrillation, RNA sequencing, Kyoto Encyclopedia of Genes and Genomes pathway, mRNA, long non-coding RNA

PersAF were identified and compared with controls. The putative function of the DE mRNAs and lncRNAs were determined by Gene Ontology (GO) and Kyoto Encyclopedia of Genes and Genomes (KEGG) pathway analyses. A co-expression network for lncRNA-mRNA was subsequently constructed. The results provide valuable molecular markers associated with the occurrence and development of ParoAF and PersAF.

Materials and methods

Patients and tissue collection. This study was permitted by the Human Ethics Committee of the First Affiliated Hospital of Nanjing Medical University (approval number: 2020-SRFA-340). All patients with AF and healthy donors provided written informed consent for the use of their tissue in this study. The informed consent of the donors was signed by one of their lineal relative members.

Patients who underwent heart transplantation in the Department of Cardiovascular Surgery at the First Affiliated Hospital of Nanjing Medical University (Nanjing, China) were recruited. Patients categorized as ParoAF and PersAF met the following criteria: i) Over 18 years old; ii) exhibited obvious symptoms of AF as confirmed by electrocardiogram and had a clear medical history; iii) minimally invasive radiofrequency ablation performed for the first time; and iv) one-lung ventilation implemented. The exclusion criteria were: i) Below 18 years old or over 70 years old; ii) unclear medical history data; iii) combined with other cardiac surgery or undergoing secondary surgery; and iv) with psychiatric illness. The donor criteria included: i) Age <50 years old, with some marginal donors <60 years old; ii) estimated cold ischemia time <8 h; iii) no long-term or repeated history of cardiopulmonary resuscitation; iv) serological examination without hepatitis B/C, acquired immunodeficiency syndrome; v) no existing bacteremia; and vi) no malignant tumors other than primary brain tumors. The exclusion criteria for donors were: i) Brain death due to cardiac arrest; ii) heart contusion; iii) intractable ventricular arrhythmia; iv) long-term or repeated cardiopulmonary resuscitation; v) past heart disease, particularly congenital heart malformations; vi) after actively optimizing the before and after load, the support of a super-large dose of inotropic drugs still needed; vii) echocardiography findings of severe heart wall motion abnormalities and reduced sustained left ventricular ejection fraction (after optimized afterload, positive muscle support and other treatments, remained 40% lower); and viii) severe left ventricular hypertrophy, with ventricular septum >13 mm and accompanied by electrocardiogram manifestations of left ventricular hypertrophy.

Left atrial appendage (LAA) tissues collected from the hearts of patients with AF (patients with ParoAF=3 and patients with PersAF=3) and donors (n=3) were used for RNA-Seq analysis. All healthy donors exhibited a sinus rhythm and were in good condition. The LAA tissues were selected from patients with ParoAF and PersAF, who underwent maze surgery. The tissues were quickly cut into pieces, placed into liquid nitrogen for at least 4 h, and then stored at -80˚C for further use.

RNA extraction. Total RNA was extracted using TRIzol reagent (Invitrogen; Thermo Fisher Scientific, Inc.) according to the manufacturer's instructions and quantified using a Qubit 3.0 (Invitrogen; Thermo Fisher Scientific, Inc.). RNA integrity (RIN) was evaluated with an Agilent 2100 Bioanalyzer (Agilent Technologies, Inc.). Samples with $OD_{260/280}$ values >1.9 and RIN >7 were used for library construction.

Whole transcriptome library preparation and sequencing. Ribosomal RNA (rRNA) was removed from the total RNA samples using the Ribo-Minus kit (Thermo Fisher Scientific, Inc.). Next, each RNA sample was quantified and used for library preparation using the TruSeq RNA Library Preparation kit version 2 (Illumina, Inc.). All libraries were loaded into one lane on the Illumina HiSeq X ten (Illumina, Inc.) platform, followed by 2x150 bp pair-end sequencing.

Bioinformatics analysis. FastQC (v0.11.5; http://www.bioinformatics.babraham.ac.uk/projects/fastqc/) was used to process the raw sequencing data. The clean reads were mapped onto the *Homo sapiens* (assembly GRCh38. P12) sequence using TopHat (v2.0.12; https://ccb.jhu.edu/software/tophat/index.shtml), followed by assembly using Cufflinks (v2.2.1; http://cufflinks.cbcb.umd.edu). Transcripts with reads per kilobase of exon per million reads mapped (RPKM>0) were retained for further analyses. EdgeR (http://www.bioconductor.org/packages/release/bioc/html/edgeR.html) was utilized to identify the DE lncRNAs and mRNAs by pairwise comparisons, using thresholds of $|\text{Log}_2$ fold change$|>2$ and $P<0.05$.

As reported, lncRNAs usually work through *cis*- and *trans*-elements (23). In the present study, the mRNAs detected by *cis* function for the DE lncRNAs were analyzed by GO (http://www.Geneontology.org/) and KEGG (http://www.genome.jp/kegg/) with a corrected $P<0.05$ considered as significantly enriched for terms and pathways, respectively. *Trans* function targeted mRNAs were predicted by correlations ≥0.9 or ≤-0.9.

mRNA-lncRNA co-expression network. The DE mRNAs upstream or downstream of the DE lncRNAs were identified and their associations were visualized using Cytoscape software (v3.6.1, https://cytoscape.org/). The DE mRNAs targeted by DE lncRNA were also calculated, and the co-expression network was displayed by Cytoscape software (v3.6.1).

Protein-protein interaction (PPI) network. The association between DE mRNAs was also revealed using a PPI network. The STRING database (https://string-db.org/cgi/input.pl) was used for an interaction correlation study and correlations of r>0.7 were displayed.

Reverse transcription-quantitative PCR (RT-qPCR). RT-qPCR was used to validate the sequencing analysis results for the DE lncRNAs and mRNAs. Expression levels of collagen, type I, alpha 1 (*COL1A1*); collagen, type I, alpha 2 (*COL2A1*); collagen, type VI, alpha 1 (*COL6A1*); dopachrome tautomerase (*DCT*); phosphodiesterase 4D, cAMP-specific (*PDE4D*); *RP11-428C19.4*; *GPC-AS2*; and *XLOC_110310* were measured in ParoAF_Control and PersAF_Control samples and normalized by β-actin expression. RNA samples were prepared as aforementioned. The primers were designed

Table I. Clinical characteristics of subjects used for the sequencing.

Characteristic	Control, n=3	ParoAF, n=3	PersAF, n=3	P-value
Age, years	39.67±1.86	53.67±3.76	57.33±3.76	0.441[a]
BMI, kg/m^2	21.70±1.62	23.07±0.55	25.17±0.44	0.059[a]
LA, mm	35.67±1.20	36.33±3.48	44.33±3.38	0.086[a]
LVDD, mm	44.33±2.73	46.67±1.20	45.33±1.33	0.429[a]
LVSD, mm	27.33±1.76	32.00±2.00	29.67±0.88	0.097[a]
Ventricular rate	56.00±4.16	91.33±8.41	73.67±8.09	0.083[a]
Systolic blood pressure	125.0±5.51	114.0±6.47	121.3±8.05	0.287[a]
Diastolic blood pressure	78.05±6.89	80.24±5.11	80.46±4.10	0.617[a]
CHA2DS2-VASc score	–	3.280±0.85	2.962±0.88	0.478[b]
HASBLED score	–	2.852±0.61	2.846±0.74	0.988[b]
EHRA	–	I(1)/II(2)	I(1)/II(2)	–

Values are expressed as means ± SEM. P≤0.05 was considered as statistically significant. [a]Difference was analyzed using non-parametric Kruskal-Wallis H test followed by Dunn's test. [b]Difference was analyzed using non-parametric Mann-Whitney U test followed by Dunn's test. CHA2DS2-VASc contains congestive heart failure/LV dysfunction, hypertension, age ≥75, diabetes mellitus, stroke/TIA/TE, vascular disease, age=65-74, and sex category. HAS-BLED contains parameters of hypertension, abnormal renal function, abnormal liver function, previous stroke, bleeding history or predisposition, history of labile international normalized ratio, age ≥65, concomitant aspirin or nonsteroidal anti-inflammatory drug therapy, and substantial alcohol intake. BMI, body mass index; LA, left atrium; LVDD, left ventricular diastolic dimension; LVEF, left ventricular ejection fraction; LVSD, left ventricular systolic diameter; EHRA, European Heart Rhythm Association; PersAF, persistent atrial fibrillation.

according to the sequences provided by the RNA-Seq data and synthesized by Genewiz Inc. (https://www.genewiz.com.cn/). The primers were provided in Table SI. RT-PCR was performed using HiScript® II One Step RT-PCR Kit (Vazyme Biotech Co., Ltd.) kit according to the manufacturer's instruction. The RT-qPCR reaction was performed using the AceQ qPCR SYBR Green Master Mix (Vazyme Biotech Co., Ltd.) with a 20 μl PCR reaction systems, including 0.5 μl of each primer (10 μM), 2 μl of cDNA, 10 μl of AceQ qPCR SYBR Green Master Mix and 7 μl of RNase free H_2O. The mixture was put on the ABI 7500 system real-time PCR instrument (Applied Biosystems, Thermo Fisher Scientific, Inc.), and the amplification conditions were as follows: Pre-denaturation at 95˚C for 30 sec; denaturation at 95˚C for 5 sec, annealing at 60˚C for 30 sec (39 cycles); extension at 95˚C for 10 sec. All the experiments were repeated in triplicate. The mRNA and lncRNA expression levels were calculated using the $2^{-\Delta\Delta Cq}$ method (24).

Statistical analysis. All statistical analyses were performed using IBM SPSS Statistics v22.0 (IBM Corp.) or GraphPad Prism 8 (GraphPad Software, Inc.) software. Normal data are shown as means ± standard error of means. Comparison among three groups was done using the non-parametric Kruskal-Wallis H test followed by Dunn's test. Comparisons between two groups were performed using the non-parametric Mann-Whitney U test. P<0.05 was considered to indicate a statistically significant difference.

Results

Clinical characteristics. There were no significant differences in age, body mass index, left ventricular diastolic dimension (LVDD), left ventricular systolic diameter, ventricular rate, systolic blood pressure and diastolic blood pressure across control donors or patients with ParoAF and PersAF (P>0.05; Table I). The CHA2DS2-VASc score (that considers congestive heart failure/LV dysfunction, hypertension, age ≥75, diabetes mellitus, stroke/TIA/TE, vascular disease, age=65-74 and sex category), HASBLED score (that considers parameters of hypertension, abnormal renal function, abnormal liver function, previous stroke, bleeding history or predisposition, history of labile international normalized ratio, age ≥65, concomitant aspirin or nonsteroidal anti-inflammatory drug therapy and substantial alcohol intake) and European Hearth Rhythm Association showed no significant differences between the ParoAF and PersAF groups.

Differentially expressed lncRNAs and mRNAs. A total of 285 (116 upregulated and 169 downregulated) and 275 (110 upregulated and 165 downregulated) DE mRNAs were identified in patients with ParoAF and PersAF compared with the control group, respectively. A total of 575 (276 upregulated and 299 downregulated) and 583 (330 upregulated and 253 downregulated) DE lncRNAs were detected in the ParoAF_Control and PersAF_Control samples, respectively. The volcano map of DE mRNAs and lncRNAs in the ParoAF_Control and PersAF_Control samples are shown in Fig. 1A-D. In addition, the expression levels of DE mRNA and lncRNAs in the ParoAF_Control and PersAF_Control samples are shown in Fig. 1E-H. The DE mRNAs and lncRNAs in the ParoAF_Control sample are provided in Tables SII and SIII, respectively, whereas the DE mRNAs and lncRNAs in the PersAF_Control samples are listed in Tables SIV and SV, respectively.

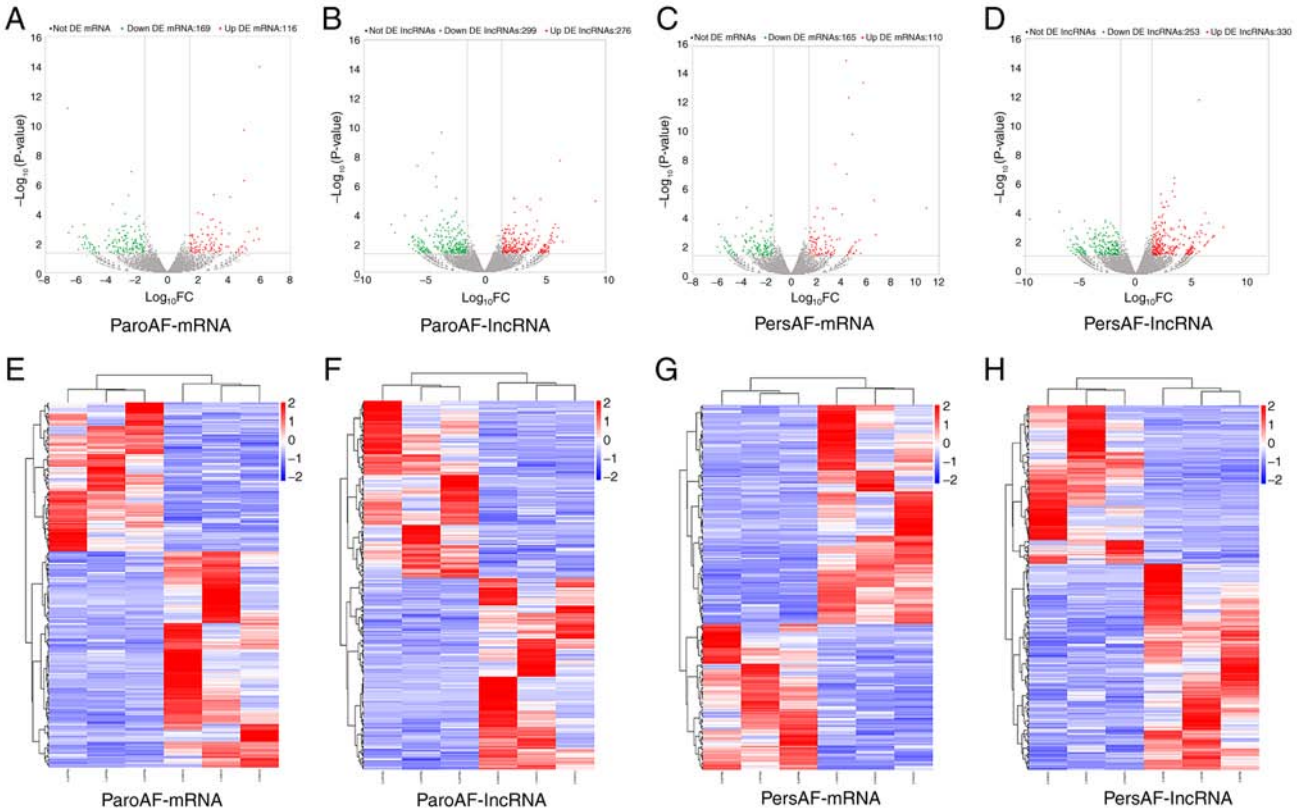

Figure 1. Expression profiles of lncRNAs and mRNAs of ParoAF and PersAF compared with control. (A-D) The volcano map of DE mRNAs and DE lncRNAs of both ParoAF and PersAF. Green represents the downregulated DE mRNAs and DE lncRNAs. Red represents the upregulated DE mRNAs and DE lncRNAs. (E-H) The heatmap of the expression levels of DE mRNAs and DE lncRNAs of ParoAF and PersAF. DE, differentially expressed; ParoAF, paroxysmal atrial fibrillation; PersAF, persistent atrial fibrillation; lncRNA, long non-coding RNA.

GO and KEGG pathway analysis of DE mRNAs. There were two GO terms for 'extracellular matrix' and 'platelet-derived growth factor binding' that were significantly enriched in the DE mRNA profile of the ParoAF_Control sample. These two GO terms were represented by *COL1A2* (upregulated), *COL6A1* (upregulated), *COL3A1* (upregulated), *COL2A1* (downregulated) and so forth. Moreover, *COL1A2* (upregulated), *COL6A1* (upregulated), and *COL3A1* (upregulated) were also significantly enriched in the GO terms 'collagen type I' and 'platelet-derived growth factor binding' in the PersAF_Control samples (Table II).

The top five enriched pathways were 'ECM-receptor interaction,' 'protein digestion and absorption,' 'PI3K-Akt signaling pathway Focal adhesion Amoebiasis,' 'TGF-beta signaling pathway,' and 'Amoebiasis' in the ParoAF_Control samples (Fig. 2A). Upregulated DE mRNAs, such as *COL1A1*, *COL1A2* and laminin β2 (*LAMB2*), were associated with most of the top ten pathways (Fig. 2C). Downregulated *COL2A1* was associated with most of the top ten pathways. Decorin (*DCN*), SMAD specific E3 ubiquitin protein ligase 2 (*SMURF2*), and interferon, γ (*IFNG*) are known to participate in the TGF-β signaling pathway.

The top five enriched pathways in the PersAF_Control were 'insulin resistance,' 'protein digestion and absorption,' 'type I diabetes mellitus,' 'herpes simplex infection,' and 'antigen processing and presentation dorso-ventral axis formation'. They were enriched in *IFNG* (upregulated), major histocompatibility complex class I C (*HLA-C*; upregulated), and interferon regulatory factor 9 (*IRF9*; downregulated) (Fig. 2B and D).

Function analysis of DE lncRNAs through cis. The upstream mRNAs of the DE lncRNAs were enriched in 'phosphoric diester hydrolase activity,' 'regulation of nucleotide metabolic process,' and 'cytoskeleton'. The GO terms 'sequence-specific DNA binding RNA polymerase II transcription factor activity,' 'response to dietary excess,' and 'positive regulation of gene expression' were enriched among the mRNAs downstream of the DE lncRNAs. The top ten GO terms of the upstream and downstream mRNAs of the DE lncRNAs are listed in Table III.

In addition, 23 and 47 KEGG pathways were enriched in upstream and downstream mRNAs respectively. The upstream mRNAs were mainly enriched in the 'Ras signaling pathway,' 'MAPK signaling pathway,' and 'PPAR signaling pathway' (Fig. 3A), whereas the downstream mRNAs were involved in 'Arrhythmogenic right ventricular cardiomyopathy,' 'Signaling pathways regulating pluripotency of stem cells,' and 'Glycine, serine and threonine metabolism' (Fig. 3B). Mitogen-activated protein kinase 10 (*MAPK10*) and phospholipase A2, group IVA (*PLA2G4A*) were involved in more pathways compared with the others for upstream DE mRNAs (Fig. 3C). For downstream mRNAs, calcium channel, voltage-dependent, L-type, alpha 1C subunit (*CACNA1C*), ATPase, Ca^{++} transporting, cardiac muscle, slow twitch 2 (*ATP2A2*), catenin (cadherin-associated protein), beta 1, 88 kDa (*CTNNB1*),

Table II. Enriched GO terms of ParoAF and PersAF when compared to control.

A, ParoAF_Control

GO terms	Term name	GO classification	Corrected P-value	Input genes
GO:0031012	Extracellular matrix	CC	$3x10^{-2}$	*COL3A1*, *COL2A1*, *THBS1*, *LAMC1*, *SPARC*, *LAD1*, *COL6A6*, *COL1A2*, *GPC1*, *THSD4*, *WISP1*, *LPL*, *ENTPD2*, *C1QTNF9B*, *LAMB2*, *IMPG1*, *TIMP4*, *ADAMTSL4*, *COL6A1*, *VCAN*, *SERPINE2*, *DCN*, *ADAM11*

B, PersAF_Control

GO terms	Term name	GO classification	Corrected P-value	Input genes
GO:0048407	Platelet-derived growth factor binding	MF	$5x10^{-3}$	*COL1A2*, *COL6A1*, *COL3A1*, *COL1A1*
GO:0005584	Collagen type I	CC	$5x10^{-2}$	*COL1A2*, *COL1A1*

GO, Gene Ontology; CC, cellular component; MF, molecular function; ParoAF, paroxysmal atrial fibrillation; PersAF, persistent atrial fibrillation.

phosphatidylinositol-4,5-bisphosphate 3-kinase, catalytic subunit alpha (*PIK3CA*), and protein kinase, cAMP-dependent, catalytic, γ (*PRKACG*) involved in no less than four pathways (Fig. 3D).

mRNA-lncRNA co-expression network. The DE mRNAs nearby the DE lncRNAs were identified and are show in Fig. 4A and B. The association between DE mRNAs and lncRNAs in the ParoAF_Control were as follows: *DCT* was downstream of GPC5-AS2, methyltransferase like 15 (*METTL15*) at the downstream of BDNF-AS (Fig. 4A). The association between DE mRNAs and DE lncRNAs in PersAF_Control, including *DCT* at the downstream of *GPC5-AS2*, chromosome 21 open reading frame 90 (*C21orf90*) at the downstream of TSPEAR-AS1, and Mdm1 nuclear protein homolog (*MDM1*) at the downstream of RP11-81H14.2 (Fig. 4B).

Next, the possible target mRNAs of the DE lncRNAs (*Trans* prediction) was assessed and a total of 709 and 1,275 mRNAs were identified in ParoAF_Control and PersAF_Control, respectively. DE mRNAs that were also targeted by DE lncRNAs were selected, which are shown in Fig. 4C and D. There were 12 and 31 DE lncRNAs and DE mRNAs co-expressed in ParoAF and PersAF samples compared with the control, respectively.

The selected mRNAs were then used for an mRNA-lncRNA network analysis. The mRNA-lncRNA co-expression network of ParoAF_Control revealed that anoctamin 3 (*ANO3*) exhibited a concomitant downregulation trend with *XLOC_002352*, *XLOC_110321*, *XLOC_098657* and *XLOC_110333*. Churchill domain containing 1 (*CHURC1*) showed downregulated expression consistent with *RP11-428C19.4* (Fig. 4E). *ANO3* and *CHURC1* co-expression were also detected in the PersAF_Control. Furthermore, *CHURC1* was also found to be co-expressed with XLOC_108610. The upregulated trend was also detected, as cardiolipin synthase 1 (*CRLS1*) was associated with RP11-380f14.2, carnitine palmitoyltransferase 1C (*CPT1C*) with RP11-498P14.4, and *NFXL1* with RP11-121C2.2 (Fig. 4F).

PPI network analysis. The PPI network in ParoAF_Control and PersAF_Control is shown in Fig. 5A and B. Fig. 5A shows that *COL3A1*, *COL1A1*, secreted protein acidic cysteine-rich (*SPARC*), *COL6A1*, *COL1A2*, *DCN*, and *COL2A1* exhibited a strong interaction with another. Downregulated genes, including breast cancer 1 early onset (*BRCA1*) and *COL2A1* are key genes that may interact with many other DE mRNAs in the ParoAF_Control network (Fig. 5A).

In PersAF_Control, upregulated genes for protein tyrosine phosphatase nonreceptor type 11 (*PTPN11*), major histocompatibility complex class II DQ alpha 1 (*HLA-DQA1*), cell division cycle 25A (*CDC25A*), β-2-microglobulin (*B2M*), *COL6A1*, *COL3A1*, *SPARC*, *COL1A1* and *COL1A2*, and downregulated DE mRNAs, including cyclin-dependent kinase 2 (*CDK2*), kelch repeat and BTB (POZ) domain containing 13 (*KBTBD13*), histone deacetylase 1 (*HDAC1*), split hand/foot malformation (ectrodactyly) type 1 (*SHFM1*), F-box and leucine-rich repeat protein 19 (*FBXL19*), and ring finger protein 19A, RBR E3 ubiquitin protein ligase (*RNF19A*) are essential genes that may interact with other DE mRNAs (Fig. 5B).

Validation of differentially expressed lncRNAs and mRNAs using RT-qPCR. The expression of the DE mRNAs and lncRNAs measured by RT-qPCR exhibited a similar trend in expression consistent with that of RNA-Seq (Fig. 6). Moreover, mRNA-lncRNA co-expression interactions of *DCT* with *GPC-AS2*, and *PDE4D* with *XLOC_110310* were demonstrated.

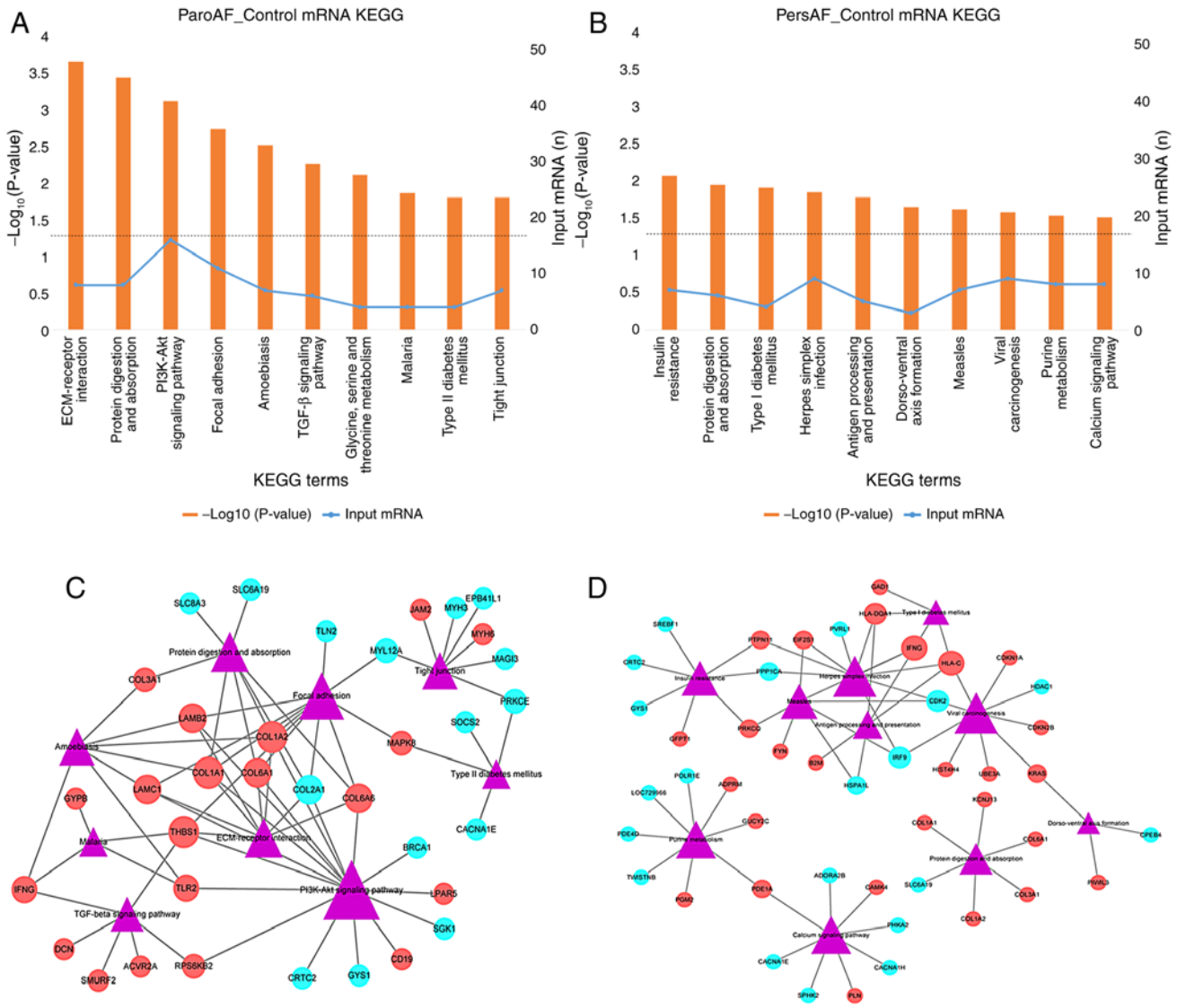

Figure 2. Top ten KEGG pathways for the DE mRNA of ParoAF and PersAF compared with control. (A and C) Bar chart and network displaying the top ten KEGG pathways of ParoAF_Control and (B and D) PersAF_Control. The dotted line in A and B represents the P=0.05, and the bar exceeding the line has a P≤0.05. The purple tringle node in C and D represents pathways, the red circle node represents the upregulated DE mRNAs, and the blue circle node represents the downregulated DE mRNAs. The number of lines decided the size of pathways and mRNAs. DE, differentially expressed; ParoAF, paroxysmal atrial fibrillation; PersAF, persistent atrial fibrillation; KEGG, Kyoto Encyclopedia of Genes and Genomes.

Discussion

AF is the most prevalent heart disease worldwide, with different subtypes causing different clinical features. Therefore, these subtypes should be treated differently. In recent years, the molecular mechanism of AF has been studied in a variety of ways. However, the studies on the differences of lncRNAs and mRNAs between ParoAF and PersAF have not been sufficient. In the present study, ParoAF, PersAF and healthy donors samples were sequenced, and found that DE mRNAs and lncRNAs vary considerably. The putative function of DE mRNAs and DE lncRNA in ParoAF_Control and PersAF_Control were also different.

COL1A2, was associated with platelet-derived growth factor binding in the comparison of both ParoAF_Control and PersAF_Control. Moreover, *COL1A2* and *COL2A1* were also associated with most of the top ten KEGG pathways in patients with ParoAF. In a study by Zhou *et al* (25), upregulated *COL1A2* in patients with AF were observed when compared with a control, suggesting that it may participate in the occurrence and development of AF. Gambini *et al* (26) demonstrated that TGF-β1 could induce the upregulation of *COL1A2* in human cardiac mesenchymal progenitor cells from PersAF specimens. The expression level of *COL1A2* in these two studies was consistent with that of the present results. In the study by Dawson *et al* (11), it was reported that *COL1A2* was a target of miR29, which may play a role in atrial fibrotic remodeling and is considered to be a biomarker or therapeutic target. In the present study, *COL1A2* also exhibited a strong connection with other recombinant collagen type I, III and IV family proteins, as determined by PPI analysis. These results suggest an important role for *COL1A2* in the pathophysiology of both patients with ParoAF and PersAF.

The PI3K/Akt and TGF-β signaling pathways were significantly enriched in the ParoAF_Control, whereas the calcium signaling pathway was significantly enriched in the PersAF_Control. Studies have demonstrated that some herbs can

Table III. Top ten GO terms for *cis* target genes of upstream and downstream DE lncRNAs.

A, Upstream

GO Terms	Term name	Corrected P-value	Input genes[a]
GO:0008081_MF	Phosphoric diester hydrolase activity	$5.73x10^{-6}$	*PLCXD3*, *PDE7B*, *GPCPD1*, *ENPP2*, *PDE5A*, *PDE3A*, *LOC101928269*, *PLCH1*, *CHRM3*, *PLCD1*
GO:0006140_BP	Regulation of nucleotide metabolic process	$1.6x10^{-4}$	*ITGB1*, *ADRB2*, *MCF2L2*, *RIN3*, *ARHGAP24*, *NF1*, *CRHR1*, *BPGM*, *RASAL2*, *GRM3*
GO:0005856_CC	Cytoskeleton	$3.9x10^{-4}$	*GRM3*, *HSPB7*, *ATP6V1D*, *BCL10*, *MPLKIP*, *CTNNB1*, *PCGF5*, *RILPL1*, *NFE2L2*, *FRMD4A*
GO:0042995_CC	Cell projection	$5x10^{-4}$	*RILPL1*, *CTNNB1*, *SPG11*, *TIAM2*, *FAM49A*, *GRM3*, *ATP6V1D*, *NF1*, *ARHGAP24*, *UNC13B*
GO:1900542_BP	Regulation of purine nucleotide metabolic process	$5x10^{-4}$	*HTR1B*, *FBXO8*, *BCAS3*, *ABR*, *MYO9A*, *BCAR3*, *RAP1B*, *ARF4*, *NRG4*, *NTRK2*
GO:0043005_CC	Neuron projection	$5.9x10^{-4}$	*APC*, *AMFR*, *NTRK2*, *PDE5A*, *PRSS23*, *ANK3*, *KCNIP1*, *SEMA6A*, *CAMK1G*, *DLG2*
GO:1901701_BP	Cellular response to oxygen-containing compound	$7.1x10^{-4}$	*TGFB1*, *PIK3CA*, *CALCRL*, *PDE4D*, *RORA*, *WDTC1*, *ATP6V1D*, *CTNNB1*, *FZD4*, *CMPK2*
GO:0008092_MF	Cytoskeletal protein binding	$1.05x10^{-3}$	*DAAM1*, *PPARGC1A*, *NCK2*, *DST*, *SHROOM3*, *DYNLL1*, *MYRIP*, *ACTR3C*, *ITGB1*, *XIRP2*
GO:0045202_CC	Synapse	$1.41x10^{-3}$	*CLSTN1*, *GRM1*, *CAMK2D*, *SYNE1*, *SLC30A3*, *UNC13B*, *RIMS4*, *CACNA1C*, *ITGB1*, *SPG11*
GO:0048731_BP	System development	$1.63x10^{-3}$	*ARHGAP24*, *ADAMTS18*, *MAPK10*, *UNC13B*, *ITGB1*, *SPG11*, *SYCP2*, *COL18A1*, *PLK5*, *FGF14*

B, Downstream

GO Terms	Term name	Corrected P-value	Input genes[a]
GO:0000981_MF	Sequence-specific DNA binding RNA polymerase II transcription factor activity	$3.12x10^{-5}$	*TGIF1*, *ZSCAN5A*, *RORA*, *NFE2L2*, *ERG*, *GATA6*, *CSRNP3*, *RDH13*, *NFIB*, *ZBTB16*
GO:0002021_BP	Response to dietary excess	$1x10^{-4}$	*BMP8A*, *TBL1XR1*, *ADRB2*, *RMI1*, *CCKAR*, *PPARGC1A*, *MC4R*
GO:0010628_BP	Positive regulation of gene expression	$2.2x10^{-4}$	*HIF1A*, *FOXD2*, *MED12L*, *NFIA*, *GTF2F2*, *TFAP2C*, *HIPK2*, *MAPK10*, *FGF7*, *TLR2*
GO:1902531_BP	Regulation of intracellular signal transduction	$6.5x10^{-4}$	*C12orf60*, *PDGFD*, *TAOK3*, *MTA3*, *FOXM1*, *MCF2L2*, *EPHB1*, *MUL1*, *OTUD7A*, *TBPL1*
GO:0045893_BP	Positive regulation of transcription, DNA-dependent	$2.33x10^{-3}$	*ARF4*, *GATA6*, *TET2*, *BCL9*, *TBL1XR1*, *BCL10*, *BCAS3*, *NFE2L2*, *SMARCA2*, *ZBTB17*
GO:1902532_BP	Negative regulation of intracellular signal transduction	$2.42x10^{-3}$	*SORL1*, *SPRED2*, *NF1*, *VGLL4*, *RORA*, *NFE2L2*, *RDH13*, *VDAC2*, *CNKSR3*, *TIMP3*
GO:0000977_MF	RNA polymerase II regulatory region sequence-specific DNA binding	$4.8x10^{-3}$	*NHLH2*, *ZNF486*, *ZNF812*, *AEBP2*, *E2F8*, *NFIA*, *FOXD2*, *ZNF736*, *MTA3*, *ZNF98*
GO:0001012_MF	RNA polymerase II regulatory region DNA binding	$5.22x10^{-3}$	*FBXO16*, *ZNF506*, *ZBTB16*, *NFIB*, *SMARCC2*, *RORA*, *ZNF708*, *NFE2L2*, *TGIF1*, *GATA6*
GO:0045944_BP	Positive regulation of transcription from RNA polymerase II promoter	$6.37x10^{-3}$	*RDH13*, *CSRNP3*, *CTNNB1*, *ADRB2*, *TMEM173*, *TGFB3*, *ATXN7*, *SMARCA2*, *NFIB*, *TET2*
GO:0001071_MF	Nucleic acid binding transcription factor activity	$8.72x10^{-3}$	*HIF1A*, *C12orf60*, *NFIA*, *FOXD2*, *TBX20*, *EPAS1*, *MTA3*, *ZNF98*, *AEBP2*

[a]List genes no more than ten. GO, Gene Ontology; CC, cellular component; MF, molecular function; BP, biological process; DE, differentially expressed; ParoAF, paroxysmal atrial fibrillation; PersAF, persistent atrial fibrillation.

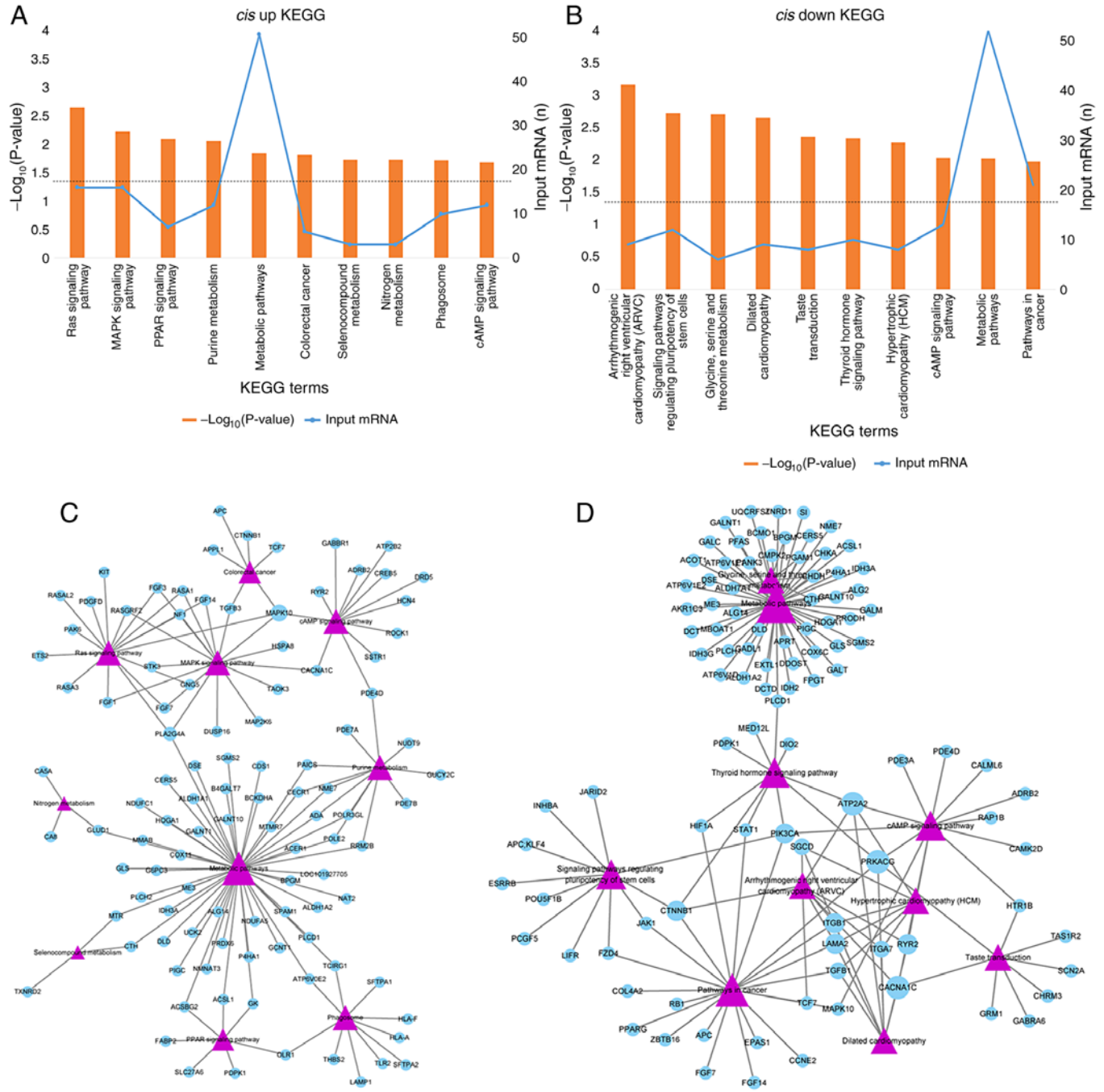

Figure 3. Top ten KEGG pathways for the *cis* analysis of upstream and downstream mRNAs of DE lncRNAs. (A and C) The bar chart and network display the top ten KEGG pathways of upstream mRNAs and (B and D) downstream mRNAs. The dotted line in A and B represents the P=0.05, and the bar exceeding the line has a P≤0.05. The purple tringle node in C and D represents pathways, and the circle node represents mRNAs. The number of lines decided the size of pathways and mRNAs. DE, differentially expressed; ParoAF, paroxysmal atrial fibrillation; PersAF, persistent atrial fibrillation; KEGG, Kyoto Encyclopedia of Genes and Genomes.

decrease the incidence of AF through the PI3K/Akt signaling pathway (27,28). Other studies have revealed that activating this pathway may reverse atrial remodeling and inhibit the occurrence of AF (29,30). Most collagen family genes detected in the present study were associated with enriched pathways of both the ParoAF_Control and PersAF_Control. Of note, *COL2A1* was only downregulated in the ParoAF_Control and is involved in PI3K-Akt signaling pathway. However, there have been no reports describing any associations among *COL2A1*, ParoAF and the PI3K/Akt signaling pathway.

TGF-β signaling is involved in the course of atrial structural remodeling in AF and is associated with the occurrence and maintenance of AF (31). Fu *et al* (32) showed that overexpressed Gal-3 in AF could subsequently activate the TGF-β1/α-SMA/Col I pathway in cardiac fibroblasts, thus strengthening atrial fibrosis. Moreover, suppressing the overexpression of TGF-β could prevent atrial remodeling (33-35). TGF-β has also been demonstrated to be a promising therapeutic target for decreasing cardiac fibrosis (36). In the present study, the TGF-β signaling pathway was significantly enriched in the ParoAF_Control

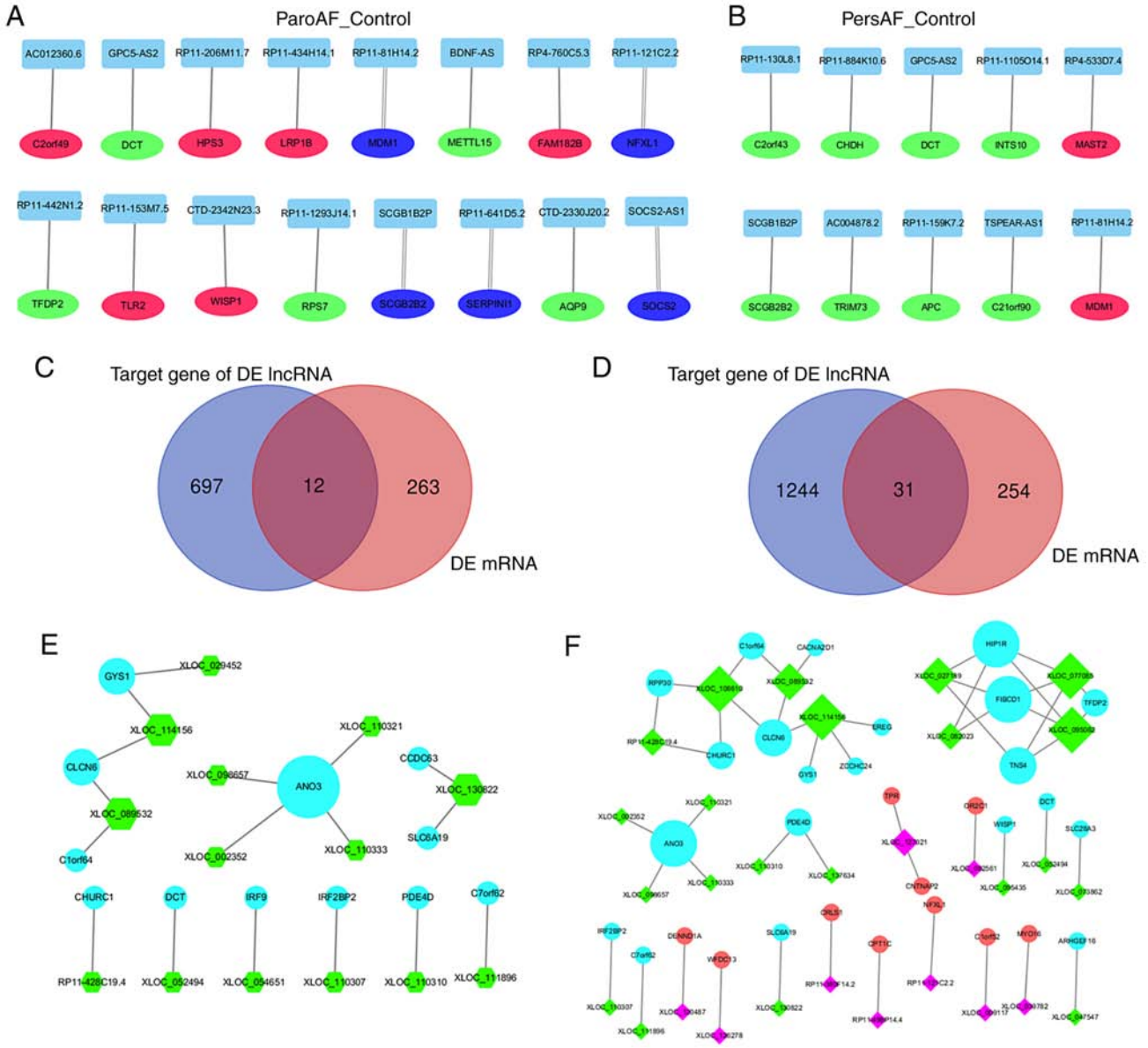

Figure 4. mRNA and lncRNA interaction co-expression network of ParoAF_Control and PersAF_Control. (A and B) DE lncRNAs and their upstream or downstream DE mRNAs. The red circle node, green circle node, and blue represents the upstream DE mRNAs, downstream DE mRNAs, and the DE mRNAs that were both upstream and downstream, respectively. The double line indicates that the DE mRNAs passes through the DE lncRNAs. The Venn map in (C and D) showed the number of target genes of DE lncRNA and DE mRNAs of ParoAF_Control and PersAF_Control, respectively. (E and F) The co-expression network of DE lncRNA and DE mRNAs of ParoAF_Control and PersAF_Control, respectively. The 'diamond node' represents DE lncRNAs, and 'circles node' represent as mRNAs. The rose-red and green colors represent upregulated and downregulated DE lncRNAs, respectively. The red and blue represent upregulated and downregulated DE mRNAs, respectively. The size of the node in A, B, E and F all represent the DE lncRNAs or DE mRNAs that were connected. DE, differentially expressed; ParoAF, paroxysmal atrial fibrillation; PersAF, persistent atrial fibrillation; lncRNA, long non-coding RNA.

along with *SMURF2* and *DCN*. *SMURF2*, which was upregulated in the present study, can induce proteasomal degradation of Smad7 and activate the TGF-β signaling pathway (37,38). *DCN*, a proteoglycan that can bind to collagen fibrils in the ECM (extracellular matrix), interacts with many growth factors, and inhibits TGF-β activity (37). Moreover, *DCN* exhibited a strong connection with other DE mRNAs in the PPI analysis in the present study. Taken together, it was hypothesized that the TGF-β signaling pathway and *DCN* may play essential roles in AF occurrence and maintenance. Moreover, TGF-β may represent an inhibitor for preventing AF occurrence.

In the present study, the calcium signaling pathway was significantly enriched in the PersAF_Control. Calcium signaling pathway was considered to play a vital role in electrical remodeling and promoting the recurrence of AF (39). Tan *et al* (38) have demonstrated that the lncRNA *HOTAIR* was involved in the modulation of calcium homeostasis in human cardiomyocytes. It was also confirmed that *HOTAIR* inhibited intracellular Ca^{2+} content by regulating L-type calcium channels. In a study on mice with ParoAF and PersAF (40), PersAF mice exhibited a phenomenon of enhanced diastolic Ca^{2+} release, marked conduction abnormalities and atrial enlargement. The absence of *PLN* increased Ca^{2+} transient amplitude and a faster Ca^{2+} decay rate (39). The combined results of these studies with the present study indicate that the calcium signaling pathway may play an essential role in the processing

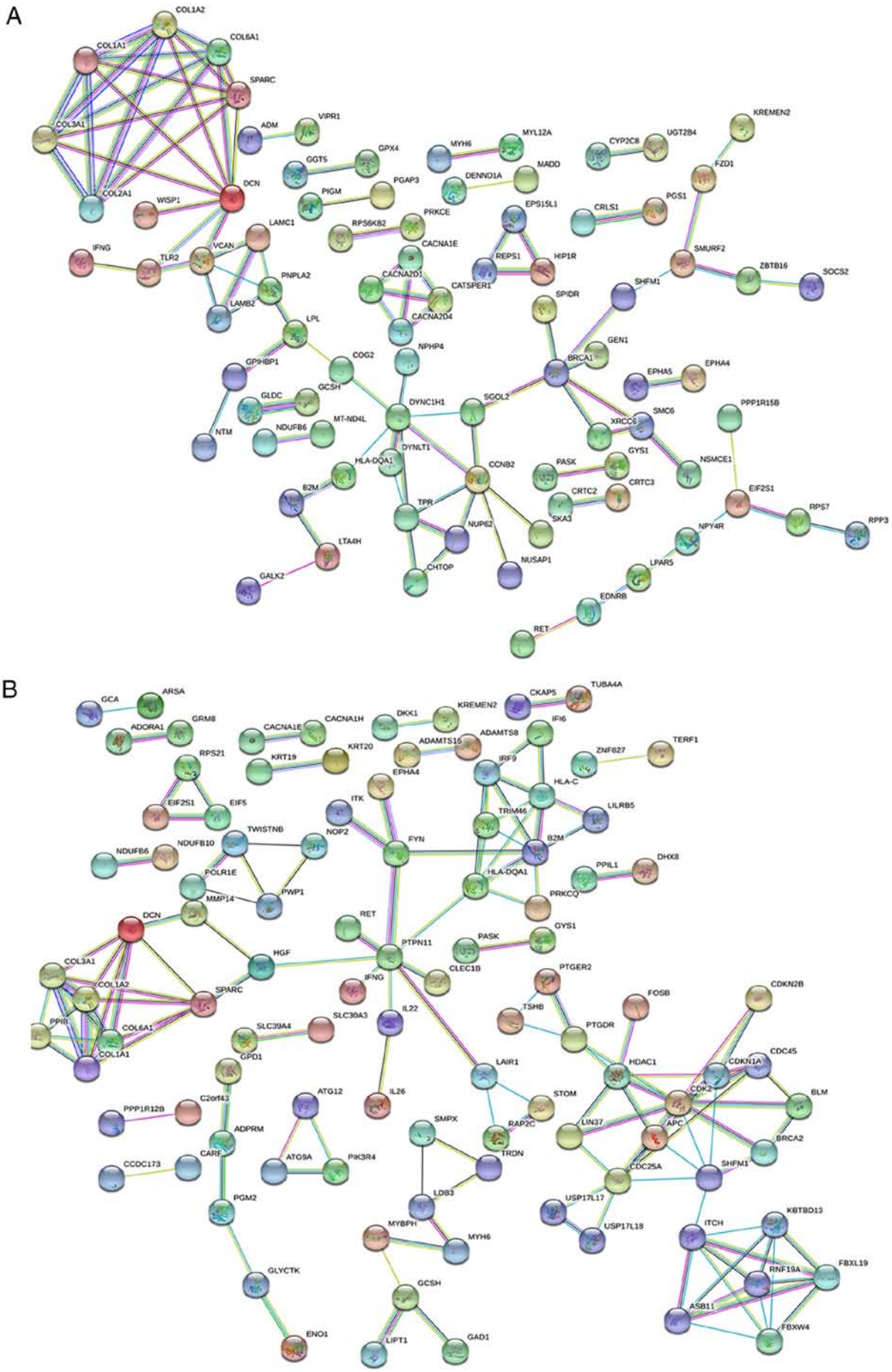

Figure 5. The protein-protein interaction network of ParoAF_Control and Pers_Control. (A) The protein-protein interaction network of ParoAF_Control. (B) The protein-protein interaction network of Pers_Control. The more lines connected, the stronger the interaction between the two mRNAs.ParoAF, paroxysmal atrial fibrillation; PersAF, persistent atrial fibrillation.

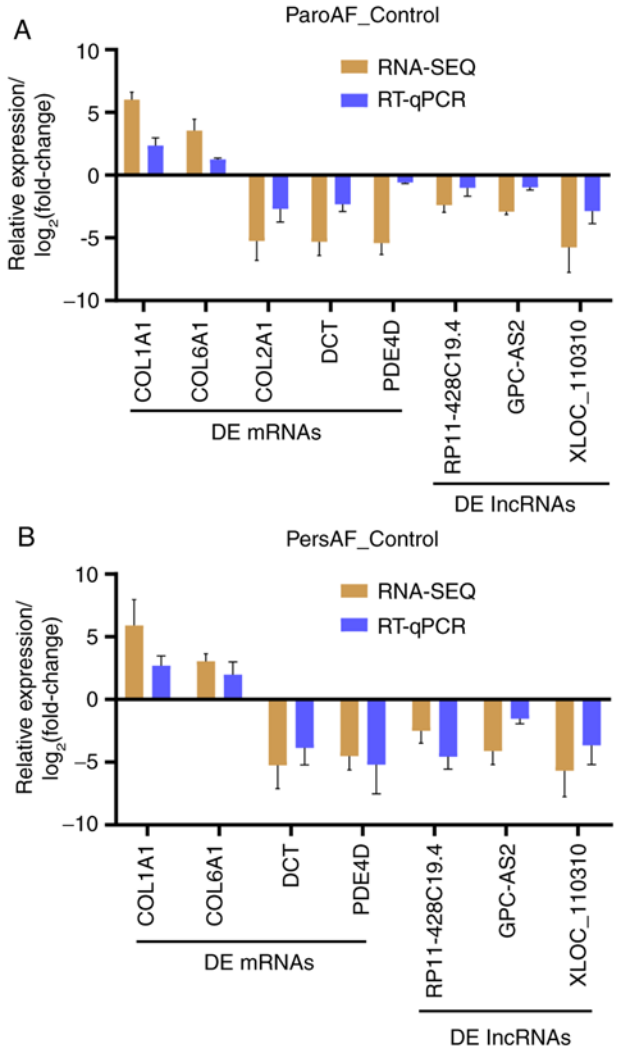

Figure 6. RT-qPCR validation of DE mRNAs and DE lncRNAs. (A) The RT-qPCR validation analysis in ParoAF. (B) The RT-qPCR validation analysis in PersAF. DE, differentially expressed; ParoAF, paroxysmal atrial fibrillation; PersAF, persistent atrial fibrillation; RT-qPCR, reverse transcription-quantitative PCR; lncRNA, long non-coding RNA..

of ParoAF to PersAF. Moreover, it was hypothesized that developing inhibitors to this pathway may inhibit the ParoAF to PersAF transition. Unfortunately, the study did not provide detailed information regarding ParoAF and PersAF and was not conducive for the comparison analysis.

lncRNAs play essential roles in ParoAF and PersAF through *cis*-elements. In the present study, *DCT* interacted with *GPC5-AS2*, and *METTL15* interacted with *BDNF-AS* in the ParoAF_Control. *DCT* interacted with *GPC5-AS2*, *C21orf90* interacted with *TSPEAR-AS1*, and *MDM1* interacted with *RP11-81H14.2* in the PersAF_Control. These DE lncRNAs may perform their function through nearby DE mRNAs. Levin *et al* (41) revealed that adult mice lacking *DCT* display normal cardiac development but an increased susceptibility to atrial arrhythmias. This suggests that lncRNA *GPC-AS2* inhibits the expression of *DCT* to influence atrial arrhythmias, which warrants further study. Through our *trans* analysis, mRNAs that were differentially expressed and targeted DE lncRNAs were identified. These DE mRNAs exhibited co-expression with DE lncRNAs. *PDE4D*, a biomarker of myocardial infarction and heart failure (42), was downregulated in both ParoAF_Control and PersAF_Control and was targeted by the DE lncRNAs of *XLOC_110310* and *XLOC_137634*. Further studies are needed to understand the molecular mechanism of DE mRNA and lncRNA interactions.

The function of DE lncRNAs in ParoAF_Control and PersAF_Control was analyzed through *cis*-elements. As a nearby gene of DE lncRNAs, *CACNA1C* was enriched in both the MAPK and cAMP signaling pathways. Zhang *et al* (43) revealed that the MAPKs/TGF-β1/TRAF6 signaling pathways participate in atrial fibrosis in patients with rheumatic heart disease, causing the occurrence of AF following cardiac surgery. Inhibiting the MAPK pathways can prevent atrial parasympathetic remodeling and the occurrence of AF (44). The induction of AF and structural remodeling was associated with MAPK expression and the decrease in collagenase activity (15). *CACNA1C* is enriched in the MAPK signal pathway which is the direct target gene of miR-29a-3p. Zhao *et al* (45) found that decreased expression of *CACNA1C* caused by overexpression of microRNA-29a underlies the pathogenesis of AF. Thus, it was assumed that miR-29a-3p may be a potential therapeutic target in AF. These studies combined with the present result indicate that the MAPK signaling pathway is an important pathway that participates in AF occurrence by preventing atrial parasympathetic remodeling.

There were some limitations in the present study. Firstly, the original intention was to study the molecular mechanism of all AF types including permanent AF, ParoAF and PersAF. However, the permanent AF samples were difficult to collect. Secondly, the sample number used in the present study was low, as more than five would have been better. Thirdly, the present study lacked functional verification of the mRNAs and lncRNAs, which will be the subject of a future study.

The present study analyzed the DE mRNAs and lncRNAs and their putative roles in ParoAF and PersAF. It was found that PI3K/Akt and TGF-β signaling were significantly enriched in the ParoAF_Control, and the calcium signaling pathway was significantly enriched in the PersAF_Control. The *cis* and *trans* analyses revealed some important interactions between DE mRNAs and lncRNAs including *GPC-AS2* with *DCT*, and *PDE4D* with *XLOC_110310* and *XLOC_137634*. In summary, the present study provided molecular theoretical data for further clinical studies involving ParoAF and PersAF.

Acknowledgements

Not applicable.

Funding

Not applicable.

Availability of data and materials

The raw data were deposited on the NCBI Sequence Read Archive (SRA), with the SRA accession number of PRJNA531935.

Authors' contributions

HS designed the study, collected the samples, conducted the experiment, analyzed the data, and wrote the manuscript. YS equally designed the study, analyzed the data, provided the foundation and revised the manuscript. Both authors read and approved the final manuscript.

Ethics approval and consent to participate

This study was permitted by the Human Ethics Committee of the Jiangsu People Hospital, (approval number, 2020-SRFA-340). All patients with AF and control patients have been informed of writing consent to use their tissue for this study.

Patient consent for publication

Not applicable.

Competing interests

The authors declare that they have no competing interests.

References

1. Marrouche NF, Brachmann J, Andresen D, Siebels J, Boersma L, Jordaens L, Merkely B, Pokushalov E, Sanders P, Proff J, *et al*: Catheter ablation for atrial fibrillation with heart failure. N Engl J Med 378: 417-427, 2018.
2. Kalman JM, Sanders P, Rosso R and Calkins H: Should we perform catheter ablation for asymptomatic atrial fibrillation? Circulation 136: 490-499, 2017.
3. Zoni Berisso M, Landolina M, Ermini G, Parretti D, Zingarini GL, Degli Esposti L, Cricelli C and Boriani G: The cost of atrial fibrillation in Italy: A five-year analysis of healthcare expenditure in the general population. From the Italian survey of atrial fibrillation management (ISAF) study. Eur Rev Med Pharmacol Sci 21: 175-183, 2017.
4. Hu CY, Wang CY, Li JY, Ma J and Li ZQ: Relationship between atrial fibrillation and heart failure. Eur Rev Med Pharmacol Sci 20: 4593-4600, 2016.
5. Yang S, Mei B, Feng K, Lin W, Chen G, Liang M, Zhang X and Wu Z: Long-term results of surgical atrial fibrillation radiofrequency ablation: Comparison of two methods. Heart Lung Circ 27: 621-628, 2018.
6. Zhao L, Wang WYS and Yang X: Anticoagulation in atrial fibrillation with heart failure. Heart Fail Rev 23: 563-571, 2018.
7. Heijman J, Voigt N, Nattel S and Dobrev D: Cellular and molecular electrophysiology of atrial fibrillation initiation, maintenance, and progression. Circ Res 114: 1483-1499, 2014.
8. Schotten U, Dobrev D, Platonov P, Kottkamp H and Hindricks G: Current controversies in determining the main mechanisms of atrial fibrillation. J Intern Med 279: 428-438, 2016.
9. Liu H, Chen GX, Liang MY, Qin H, Rong J, Yao JP and Wu ZK: Atrial fibrillation alters the microRNA expression profiles of the left atria of patients with mitral stenosis. BMC Cardiovasc Disord 14: 10, 2014.
10. Yubing W, Yanping X, Zhiyu L, Weijie C, Li S, Huaan D, Peilin X, Zengzhang L abd Yuehui Y: Long-term outcome of radiofrequency catheter ablation for persistent atrial fibrillation. Medicine (Baltimore) 97: e11520, 2018.
11. Dawson K, Wakili R, Ördög B, Clauss S, Chen Y, Iwasaki Y, Voigt N, Qi XY, Sinner MF, Dobrev D, *et al*: MicroRNA29: A mechanistic contributor and potential biomarker in atrial fibrillation. Circulation 127: 1466-1475, 1475e1-28, 2013.
12. McManus DD, Lin H, Tanriverdi K, Quercio M, Yin X, Larson MG, Ellinor PT, Levy D, Freedman JE and Benjamin EJ: Relations between circulating microRNAs and atrial fibrillation: Data from the Framingham offspring study. Heart Rhythm 11: 663-669, 2014.
13. Wang Y, Cai H, Li H, Gao Z and Song K: Atrial overexpression of microRNA-27b attenuates angiotensin II-induced atrial fibrosis and fibrillation by targeting ALK5. Hum Cell 31: 251-260, 2018.
14. Saxena A and Carninci P: Long non-coding RNA modifies chromatin: Epigenetic silencing by long non-coding RNAs. Bioessays 33: 830-839, 2011.
15. Ruan Z, Sun X, Sheng H and Zhu L: Long non-coding RNA expression profile in atrial fibrillation. Int J Clin Exp Pathol 8: 8402-8410, 2015.
16. Song C, Zhang J, Liu Y, Pan H, Qi HP, Cao YG, Zhao JM, Li S, Guo J, Sun HL and Li CQ: Construction and analysis of cardiac hypertrophy-associated lncRNA-mRNA network based on competitive endogenous RNA reveal functional lncRNAs in cardiac hypertrophy. Oncotarget 7: 10827-10840, 2016.
17. Liang H, Pan Z, Zhao X, Liu L, Sun J, Su X, Xu C, Zhou Y, Zhao D, Xu B, *et al*: lncRNA PFL contributes to cardiac fibrosis by acting as a competing endogenous RNA of let-7d. Theranostics 8: 1180-1194, 2018.
18. Chen G, Guo H, Song Y, Chang H, Wang S, Zhang M and Liu C: Long non-coding RNA AK055347 is upregulated in patients with atrial fibrillation and regulates mitochondrial energy production in myocardiocytes. Mol Med Rep 14: 5311-5317, 2016.
19. Chen L, Yan KP, Liu XC, Wang W, Li C, Li M and Qiu CG: Valsartan regulates TGF-β/Smads and TGF-β/p38 pathways through lncRNA CHRF to improve doxorubicin-induced heart failure. Arch Pharm Res 41: 101-109, 2018.
20. Su Y, Li L, Zhao S, Yue Y and Yang S: The long noncoding RNA expression profiles of paroxysmal atrial fibrillation identified by microarray analysis. Gene 642: 125-134, 2018.
21. Yu XJ, Zou LH, Jin JH, Xiao F, Li L, Liu N, Yang JF and Zou T: Long noncoding RNAs and novel inflammatory genes determined by RNA sequencing in human lymphocytes are up-regulated in permanent atrial fibrillation. Am J Transl Res 9: 2314-2336, 2017.
22. Chiang DY, Zhang M, Voigt N, Alsina KM, Jakob H, Martin JF, Dobrev D, Wehrens XHT and Li N: Identification of microRNA-mRNA dysregulations in paroxysmal atrial fibrillation. Int J Cardiol 184: 190-197, 2015.
23. Paralkar VR, Taborda CC, Huang P, Yao Y, Kossenkov AV, Prasad R, Luan J, Davies JO, Hughes JR, Hardison RC, *et al*: Unlinking an lncRNA from its associated *cis* element. Mol Cell 62: 104-110, 2016.
24. Schmittgen TD and Livak KJ: Analyzing real-time PCR data by the comparative C(T) method. Nat Protoc 3: 1101-1108, 2008.
25. Zhou DD, Jiang YY, Yuan C and Shi C: A study on expression and distribution of collagen in rheumatic heart disease with atrial fibrillation. Guangdong Med J, 2017.
26. Gambini E, Perrucci GL, Bassetti B, Spaltro G, Campostrini G, Lionetti MC, Pilozzi A, Martinelli F, Farruggia A, DiFrancesco D, *et al*: Preferential myofibroblast differentiation of cardiac mesenchymal progenitor cells in the presence of atrial fibrillation. Transl Res 192: 54-67, 2018.
27. Mao T, Zhang J, Qiao Y, Liu B and Zhang S: Uncovering synergistic mechanism of Chinese herbal medicine in the treatment of atrial fibrillation with obstructive sleep apnea hypopnea syndrome by network pharmacology. Evid Based Complement Alternat Med 2019: 8691608, 2019.
28. Chong E, Chang SL, Hsiao YW, Singhal R, Liu SH, Leha T, Lin WY, Hsu CP, Chen YC, Chen YJ, *et al*: Resveratrol, a red wine antioxidant, reduces atrial fibrillation susceptibility in the failing heart by PI3K/AKT/eNOS signaling pathway activation. Heart Rhythm 12: 1046-1056, 2015.
29. Liu SH, Hsiao YW, Chong E, Singhal R, Fong MC, Tsai YN, Hsu CP, Chen YC, Chen YJ, Chiou CW, *et al*: Rhodiola inhibits atrial arrhythmogenesis in a heart failure model. J Cardiovasc Electrophysiol 27: 1093-1101, 2016.
30. Mira YE, Muhuyati, Lu WH, He PY, Liu ZQ and Yang YC: TGF-β1 signal pathway in the regulation of inflammation in patients with atrial fibrillation. Asian Pac J Trop Med 6: 999-1003, 2013.
31. Shen H, Wang J, Min J, Xi W, Gao Y, Yin L, Yu Y, Liu K, Xiao J, Zhang YF and Wang ZN: Activation of TGF-β1/α-SMA/Col I profibrotic pathway in fibroblasts by galectin-3 contributes to atrial fibrosis in experimental models and patients. Cell Physiol Biochem 47: 851-863, 2018.
32. Fu H, Li G, Liu C, Li J, Wang X, Cheng L and Liu T: Probucol prevents atrial remodeling by inhibiting oxidative stress and TNF-α/NF-κB/TGF-β signal transduction pathway in alloxan-induced diabetic rabbits. J Cardiovasc Electrophysiol 26: 211-222, 2015.
33. Verheule S, Sato T, Everett T IV, Engle SK, Otten D, Rubart-Von Der Lohe M, Nakajima HO, Nakajima H, Field LJ and Olgin JE: Increased vulnerability to atrial fibrillation in transgenic mice with selective atrial fibrosis caused by overexpression of TGF-beta1. Circ Res 94: 1458-1465, 2004.

34. He X, Zhang K, Gao X, Li L, Tan H, Chen J and Zhou Y: Rapid atrial pacing induces myocardial fibrosis by down-regulating Smad7 via microRNA-21 in rabbit. Heart Vessels 31: 1696-1708, 2016.
35. Xie J, Tu T, Zhou S and Liu Q: Transforming growth factor (TGF)-β1 signal pathway: A promising therapeutic target for attenuating cardiac fibrosis. Int J Cardiol 239: 9, 2017.
36. Cunnington RH, Nazari M and Dixon IM: c-Ski, Smurf2, and Arkadia as regulators of TGF-beta signaling: New targets for managing myofibroblast function and cardiac fibrosis. Can J Physiol Pharmacol 87: 764-772, 2009.
37. Järvinen TAH and Ruoslahti E: Generation of a multi-functional, target organ-specific, anti-fibrotic molecule by molecular engineering of the extracellular matrix protein, decorin. Br J Pharmacol 176: 16-25, 2019.
38. Tan WL, Xu M, Liu Z, Wu TY, Yang Y, Luo J, Yang J and Luo Y: HOTAIR inhibited intracellular Ca^{2+} via regulation of Cav1.2 channel in human cardiomyocytes. Cell Mol Biol (Noisy-le-grand) 61: 79-83, 2015.
39. Baskin KK, Makarewich CA, DeLeon SM, Ye W, Chen B, Beetz N, Schrewe H, Bassel-Duby R and Olson EN: MED12 regulates a transcriptional network of calcium-handling genes in the heart. JCI Insight 2: e91920, 2017.
40. Li N, Chiang DY, Wang S, Wang Q, Sun L, Voigt N, Respress JL, Ather S, Skapura DG, Jordan VK, *et al*: Ryanodine receptor-mediated calcium leak drives progressive development of an atrial fibrillation substrate in a transgenic mouse model. Circulation 129: 1276-1285, 2014.
41. Levin MD, Lu MM, Petrenko NB, Hawkins BJ, Gupta TH, Lang D, Buckley PT, Jochems J, Liu F, Spurney CF, *et al*: Melanocyte-like cells in the heart and pulmonary veins contribute to atrial arrhythmia triggers. J Clin Invest 119: 3420-3436, 2009.
42. Swyngedouw NE and Jickling GC: RNA as a stroke biomarker. Fut Neurol 12: 71-78, 2017.
43. Zhang D, Chen X, Wang Q, Wu S, Zheng Y and Liu X: Role of the MAPKs/TGF-β1/TRAF6 signaling pathway in postoperative atrial fibrillation. PLoS One 12: e0173759, 2017.
44. Liu L, Geng J, Zhao H, Yun F, Wang X, Yan S, Ding X, Li W, Wang D, Li J, *et al*: Valsartan reduced atrial fibrillation susceptibility by inhibiting atrial parasympathetic remodeling through MAPKs/neurturin pathway. Cell Physiol Biochem 36: 2039-2050, 2015.
45. Zhao Y, Yuan Y and Qiu C: Underexpression of CACNA1C caused by overexpression of microRNA-29a underlies the pathogenesis of atrial fibrillation. Med Sci Monit 22: 2175-2181, 2016.